Journal of Building Engineering 111 (2025) 113438

Contents lists available at ScienceDirect

Journal of Building Engineering

journal homepage: www.elsevier.com/locate/jobe

# A transformer-based approach for similar layout retrieval and difference detection in architectural drawings of wood frame buildings

Hao Xie [a], Qipei Mei [a,*], Ying Hei Chui [a], Haitao Yu [b]

[a] Department of Civil and Environmental Engineering, University of Alberta, Edmonton, Alberta, T6G 1H9, Canada
[b] Landmark Group of Companies, Edmonton, Canada

ARTICLE INFO

*Keywords:*
Layout drawing
Similarity
Image comparison
Deep learning
Building design

ABSTRACT

With labor shortages and increasing housing demands, efficient design methods are essential. Prefabricated buildings offer faster construction, better quality, and reduced waste. Typically, similar architectural layouts in prefabricated buildings imply comparable structural designs. Leveraging this correlation enables builders to reference previous designs, thereby reducing design time. However, manually searching databases can be time-consuming. The use of deep learning techniques can expedite this process. Through deep learning, designers can efficiently and accurately search databases for buildings with similar layouts. In this study, a drawing segmentation model was used to extract wall information from layout drawings. Buildings were then grouped into clusters based on this information. Subsequently, a pixel-wise difference method was developed to identify buildings with similar features and to highlight the differences between drawings. Finally, the proposed method was evaluated through two case studies. The results showed the proposed method can achieve acceptable accuracy in finding similar projects and identifying differences.

## 1. Introduction

As the economy progresses and living standards improve, both governments and the construction industry are increasingly focusing on prefabricated buildings for their rapid construction and energy efficiency. Prefabricated buildings are gaining popularity due to many benefits, including reduced construction time, improved quality and higher precision [1,2], compared to traditional site-built construction. These buildings are constructed by manufacturing components in the factory, which are then transported to the construction site for assembly. Notably, doors and windows are already installed in the prefabricated panels, reducing the need for additional on-site work. This streamlined construction method boosts efficiency and ensures accuracy during assembly at the construction site.

For prefabricated wood frame residential buildings, it is noted that many designs are similar to each other. Moreover, similar architectural layouts often indicate similar structural designs, particularly within the same geographical area. Using this correlation enables builders to reference previous designs, thereby minimizing the design time. However, the traditional approach of manually searching for similar designs in the database can be time-consuming. As a result, there is a growing interest in exploring deep learning

* Corresponding author.
*E-mail address:* qipei@ualberta.ca (Q. Mei).

https://doi.org/10.1016/j.jobe.2025.113438
Received 30 January 2025; Received in revised form 4 July 2025; Accepted 8 July 2025
Available online 10 July 2025

as a powerful tool to expedite the design research process. Since the emergence of deep learning, it has been applied to various aspects of structural engineering. Notable instances include its use in shear wall design [3–8], component sizing [9], and designs for beams [10,11] and braces [12,13] respectively. Deep learning can learn from previous experiences and generate optimal design solutions. Its exceptional proficiency offers a high level of accuracy and efficiency, making it an invaluable resource for designers. Deep learning can efficiently and accurately search the database for prefabricated buildings with similar features. This not only speeds up the design process but also reduces labor costs, making it an especially appealing solution amid skilled labor shortages and rising demand.

In the preliminary structural design stage of wood frame buildings, designers can modify previous designs that share significant similarities with the current project in terms of layout, rather than starting from scratch. This can be achieved by comparing architectural drawings of previous and current projects. However, the comparison process can be tedious and time-consuming. The purpose of this study is to demonstrate the effectiveness of using deep learning to identify completed buildings with similar designs and highlight differences, allowing designers to make only minor adjustments to existing designs, thereby speeding up the design process. Specifically, this study introduces a deep learning-based approach for comparing details in architectural drawings. The methodology begins with the collection of real-world engineering drawings to build a comprehensive database through segmentation using a transformer-based model, which serves as the foundation for subsequent analysis. A clustering algorithm is then applied to categorize the database into clusters, improving the organization and accessibility of the stored information. Following this, a similarity assessment method is demonstrated, enabling efficient retrieval of relevant data. The similarity is calculated based on pixel-level layout differences. When two layouts share more pixels in the same locations, fewer modifications are required, and the similarity is considered relatively high. Unlike existing retrieval methods, the proposed approach uses pixel-wise differences to efficiently search similar building layouts. Additionally, visualization techniques are introduced to highlight differences between two drawings, providing designers with valuable modification insights for further analysis and decision-making.

## 2. Related work

### 2.1. Drawing information extraction

Automatically extracting drawing information will replace the time-consuming manual process. The extracted information will enhance 3D Building Information Modeling (BIM) workflows and reduce the modeling workload [14]. Gimenez et al. [15] utilized optical character recognition (OCR) to identify and extract text elements, along with a standard Hough-based method to detect segments and arcs. Their methodology involved recognizing wall segments and openings through hand-crafted features. Recognizing the potential of deep learning, Pizarro et al. [16] conducted a review that underscored its promise in information extraction from complex visual data, providing a more automated and versatile alternative to traditional methods. In their subsequent study, U-Net [17] was utilized to extract wall objects in floor plan drawings [18]. Zeng et al. [19] proposed a method specifically for recognizing diverse elements in floor plan layouts, employing a deep multi-task neural network that incorporated a room-boundary-guided attention mechanism and a cross-and-within-task weighted loss to address multi-label tasks. Additionally, they introduced two new datasets to facilitate advancements in floor plan recognition. In the realm of structural drawings, Zhao et al. [20] presented a hybrid method leveraging image processing, Faster R-CNN [21], and OCR to extract object information. The approach aimed to generate Industry Foundation Classes (IFC) of BIM for existing buildings. Experimental results confirmed the feasibility and reliability of their method, with a detailed analysis of factors influencing accuracy. Liu et al. [22] recognized raster images by extracting junctions of walls and openings. Meanwhile, Lv et al. [23] proposed a systematic method for extracting information from layout drawings, utilizing a key points detection network and cluster analysis to extract scale information. This method contributed to a more comprehensive understanding of layout drawings, emphasizing the importance of extracting specific details for various design and analysis applications. Xu et al. [24] proposed a convolutional neural network (CNN)-based architecture that effectively detects visual objects, such as stairs. Xie et al. [25] utilized a semi-supervised learning method for building wall layout segmentation using a Swin transformer based model. With the development of Transformer models, research indicates that compared to CNNs such as U-Net [17], transformers with self-attention mechanisms have the advantage of capturing long-distance dependencies [26]. This enables more effective capture of global information, which is beneficial for wall segmentation tasks that often involve high aspect ratios. Additionally, while prior studies have primarily focused on information extraction, the construction and utilization of comprehensive databases have not received adequate attention. Beyond extracting information, further research is needed to analyze the segmentation results produced by the transformer-based model to derive meaningful insights. Therefore, this study emphasizes the analysis of segmentation outcomes after applying the advanced transformer-based model.

### 2.2. Similarity assessment

To improve the process of retrieving similar projects from a prebuilt database, the effectiveness of initiating a new project can be significantly enhanced by referring to previous projects. Park and Um [27] emphasized the strategic use of dominant shapes as crucial for retrieving 2D objects. Similarly, Fonseca and Jorge [28] developed a method for automating the indexing of technical drawing databases using geometric features and algorithms for drawing simplification. Their indexing structure was described in detail, allowing for efficient searches in extensive drawing databases. Yu and Hsu [29] presented a content-based text mining technique for efficient retrieval of CAD documents from large databases. The Content-based CAD document Retrieval System (CCRS) prototype, utilizing the Vector Space Model (VSM), retrieved relevant CAD documents, demonstrating potential for improving the retrieval and reusability of CAD documents in the construction industry.

In the specific floor plan retrieval, the work of Sharma et al. [30] introduced a CNN-based framework that facilitates the matching of floor plans. The floor plan image retrieval system proposed by Refs. [31,32] demonstrated adaptability in handling scan rotations, showcasing resilience against potential distortions introduced by scaling variations. In the field of image clustering, Xiao [33] proposed a method utilizing grating difference measures for proficient image matching and clustering. Rodrigues et al. [34] compared four architectural shape representations for unsupervised clustering on a synthetic dataset of 72 floor plans. The Tangent Distance descriptor outperformed Point Distance, Turning Function, and Grid-Based representations, yielding the highest Rand index in comparison to a reference clustering. Van Engelenburg et al. [35] developed a visually-guided Graph Edit Distance (GED) metric combined with Intersection over Union (IoU) to more accurately measure structural similarity in floor plan layouts.

Previous studies on deep learning applications for floor plans have primarily focused on identifying similar designs based on layout drawings, but they have not adequately addressed the workload of modifying model requirements nor provided clear indicators to highlight differences among drawings from similar buildings. However, minimizing the need for modifications and effectively highlighting these differences are crucial for model adjustments. They guide designers on where changes are needed and assist in decision-making. The method introduced in this paper is both automated and effective, helping designers not only to find similar drawings but also to pinpoint differences, thus offering valuable insights for subsequent detailed design phases. By focusing on prefabricated timber houses, this method addresses a research gap in this area. It aims to enhance the usability of deep learning applications by streamlining

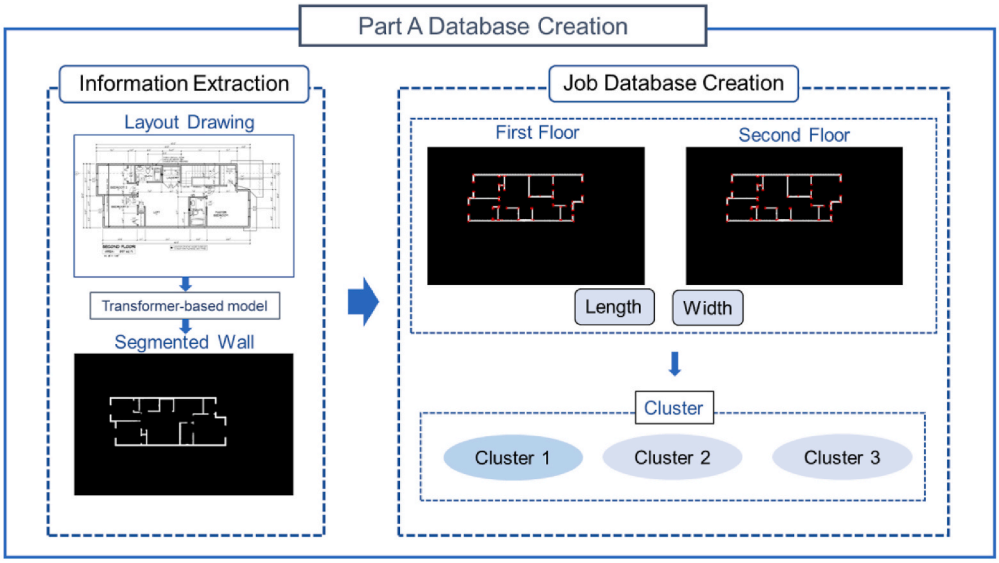


(a) Database creation

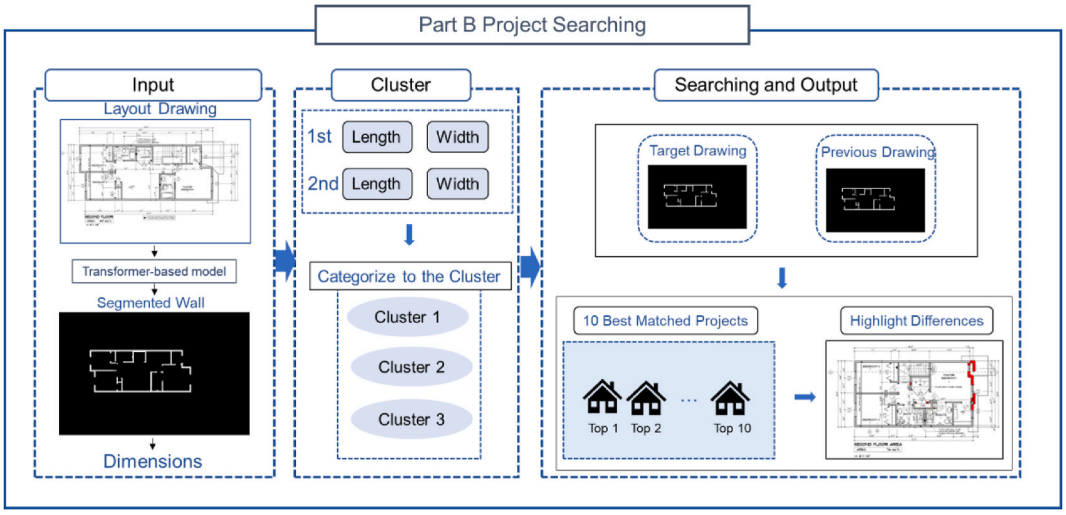


(b) Project searching

**Fig. 1.** Methodology for the best matched houses retrieval and difference highlighting.

model adjustments for specific requirements.

## 3. Methodology

This study introduces a drawing-based approach leveraging deep learning technologies for creating a database, retrieving similar house designs and highlighting differences between them. The extraction of information from previous drawings facilitated the creation of a comprehensive database. Subsequently, for new projects, the extraction, clustering, and search processes were employed to select the best matched buildings, with a particular emphasis on identifying and highlighting the differences among them. The methodology includes two main parts, as illustrated in Fig. 1.

In Fig. 1 (a), the construction of the database began with a focus on the layout drawing within each project, which plays a central role in the design process by detailing floor dimensions. Wall-related information, which is crucial for the design process, was extracted using the segmentation model Swin UNETR [36]. The shape information was then processed, and the dimensions for each house were obtained through corner detection [37]. Subsequently, these dimensions were organized into three clusters based on width and length using the K-means method, forming the basis of the database. For a detailed explanation, refer to Sections 3.2.

In Fig. 1 (b), the process for initiating a new project is outlined, focusing on identifying similar projects and highlighting differences between them. The input for this phase includes target drawings representing the new project, which undergo an initial segmentation process to obtain their dimensions. These dimensions are then used to categorize the drawings into relevant clusters. A comparison of drawings within the same cluster is conducted to compute the similarity ratio, facilitating the selection of 10 best-matched buildings for the target building. For detailed explanations, refer to Section 3.3. Finally, to aid in the model modifications, differences in the original drawings are highlighted, allowing designers to easily identify and review areas that require modifications. For more information, see Section 3.4.

### 3.1. Dataset

In this study, a total of 461 prefabricated wood frame houses were collected from a local home builder, all originally designed by professional designers. These are single-family homes consisting of two above-ground floors: a main floor and a second floor. The floor dimensions mainly range from 30 to 70 feet in length and 20–30 feet in width. These houses can typically be categorized into two main types: those with an attached garage and those with a detached garage, as illustrated in Fig. 2. Among the collected drawings, 257

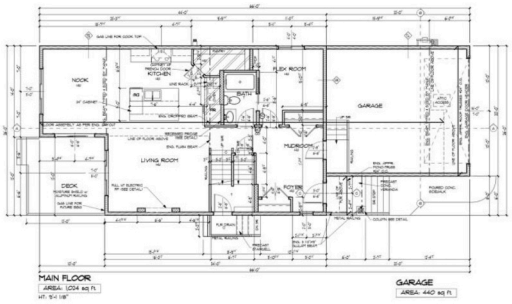


(a) Main floor of the house with an attached garage

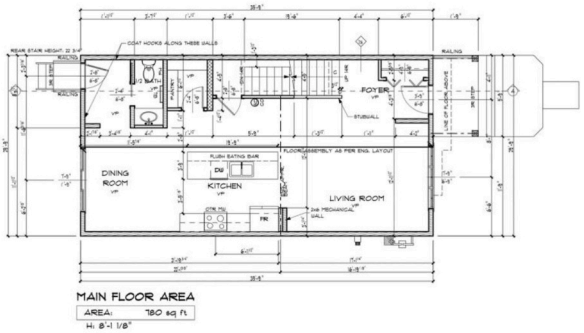


(b) Main floor of the house with a detached garage

**Fig. 2.** Representative drawings.

houses with an attached garage accounted for 55.7 % of the dataset, while the remaining 204 houses with a detached garage made up 44.3 % of the total.

For each house, the drawings of the main floor and the second floor were chosen for comparison. The basement drawings, typically showing only the exterior walls—identical to those on the main floor—were excluded from this analysis. This study involved creating a dataset to store all the projects. The deep learning model was trained to extract useful information, as detailed in Section 3.2. The training process involved annotating floor plan drawings, which are presented as binary drawings with wall features marked by distinct dark black lines, as shown in Fig. 3. Manual annotations, specifically of wall outlines, were crucial for the model's effective training. Given that the walls in the current dataset have relatively clear outlines and distinct features within the drawings, segmenting them was not overly complex. The drawings were preprocessed by cropping to remove unnecessary table blocks and then binarized. Then, 500 drawings were annotated and randomly divided into three groups: 72 % for the training dataset, 8 % for the validation dataset, and 20 % for the test dataset, as illustrated in Fig. 4. Then all drawings were then segmented using the trained Swin UNETR model [36].

### 3.2. Wall segmentation and database creation

The drawing information includes detailed wall layouts and dimensions. To segment the layout, Swin UNETR was selected due to its proven ability to capture long-range dependencies [36]. The Swin UNETR (Fig. 5) has four stages, each comprising two transformer blocks. Its U-shaped design enables the decoder to leverage the encoder's feature representations through skip connections at multiple resolutions. The Adam optimizer was selected and the learning rate was set to $10^{-4}$.

Focal loss is employed to address the extreme imbalance between foreground and background classes [38]. Since wall pixels constitute only a small fraction of the total pixels, focal loss targets the class imbalance issue, making it suited for wall segmentation.

To evaluate the performance of the model, the IoU metric was employed. mIoU represents the mean of the IoU. The IoU is calculated as shown in Eq. (1), where $c$ is the set of target pixels, $y$ is the set of ground-truth pixels, and $\widetilde{y}$ is the set of predicted pixels. The IoU metrics ranges from 0 to 1, where 0 indicates no overlap and 1 signifies perfect overlap, representing the worst and best outcomes, respectively.

$$\mathrm{IoU} = \frac{|\{y = c\} \cap \{\widetilde{y} = c\}|}{|\{y = c\} \cup \{\widetilde{y} = c\}|} \tag{1}$$

To address the potential presence of noisy points in the segmentation results, a post-processing step was implemented before corner detection. Studies suggest that morphological operations can improve the segmentation outcomes [39,40]. In this study, the drawing was processed using morphological operations [41] to eliminate these noisy points, as depicted in Fig. 6. In Fig. 6(b), the segmented picture was displayed with small white noisy points. Fig. 6(c) shows the results after applying morphological operations, effectively eliminating the noisy points and demonstrating the effectiveness of the post-processing step.

For dimension extraction, since the wall information in the results appears as shapes rather than lines, detecting the corners of each shape is crucial to obtaining accurate wall dimensions. In this study, subpixel corner detection [37] was employed to achieve this. After initially identifying Harris corners, the centroids of these corners were iteratively refined until a satisfactory level of accuracy was attained. Fig. 7 displays the corner results highlighted by red points. It is important to note that the distances represented in the corners reflect pixel distance rather than real-world measurements. However, given that all drawings in this study consistently incorporate a scale, the actual dimensions for each drawing were determined by establishing the pixel-to-actual dimension scaling.

To achieve the objective of identifying similar projects, it is not always necessary to compare projects with significant dimension differences. To address this, houses were categorized into groups based on their dimensions. This categorization was accomplished using the K-means method, an automated data clustering technique. The objective of K-means is to divide a set of $n$ observations into $k$

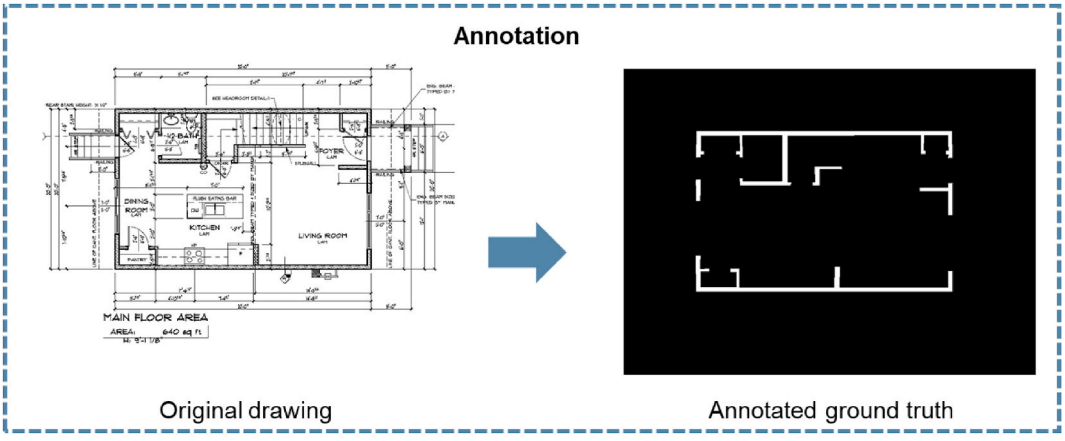


**Fig. 3.** Annotation sample.

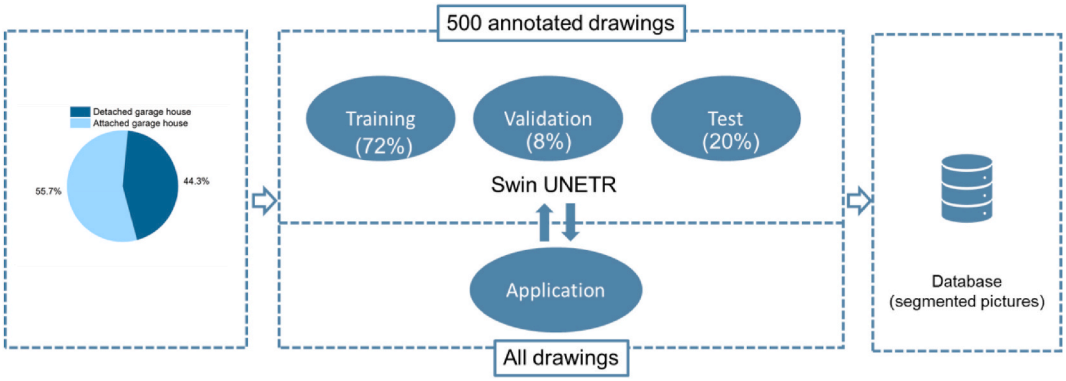


**Fig. 4.** Database creation process.

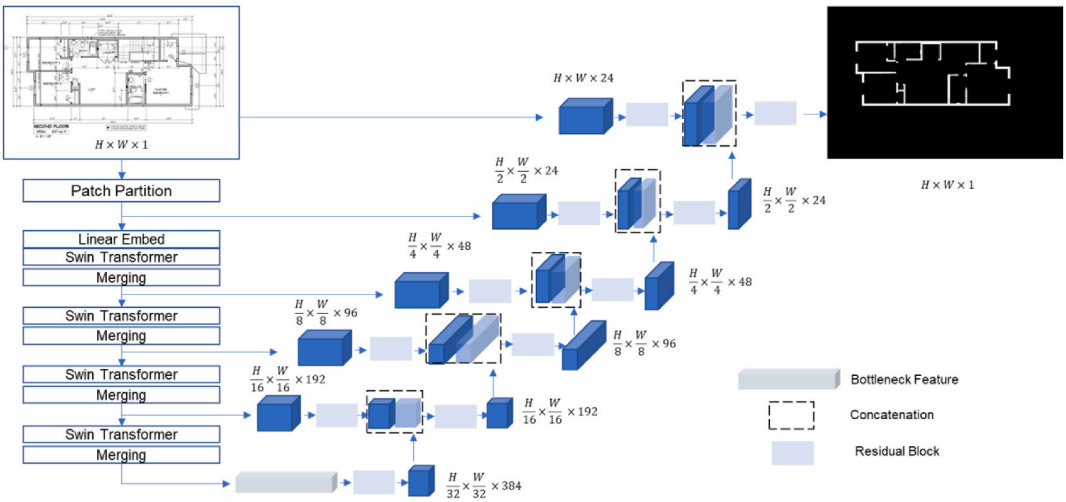


**Fig. 5.** Swin UNETR architecture [36].


**Fig. 6.** Morphological operation result.

clusters, with each observation assigned to the cluster whose mean (the cluster center or centroid) is nearest. This assignment effectively represents the typical characteristics of that cluster [42]. In this dataset, each data point was characterized by four numbers, as shown in Eq. (2). The length and width indicate the total dimension in two directions, as shown in Fig. 8. Length refers to the longer side of the building, and width refers to the shorter side. These four numbers show the total dimensions of the two floors.

$$\text{Data} = \{\text{'Main Floor Length'}, \text{'Main Floor Width'}, \text{'Second Floor Length'}, \text{'Second Floor Width'}\} \quad (2)$$

To establish the center of each cluster, the distance between the points was calculated using the Euclidean distance, as shown in Eq.

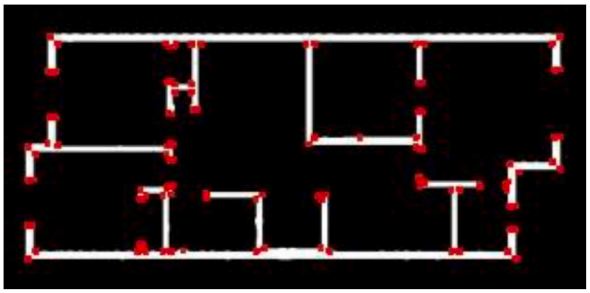

**Fig. 7.** Corner detection for dimension calculation.

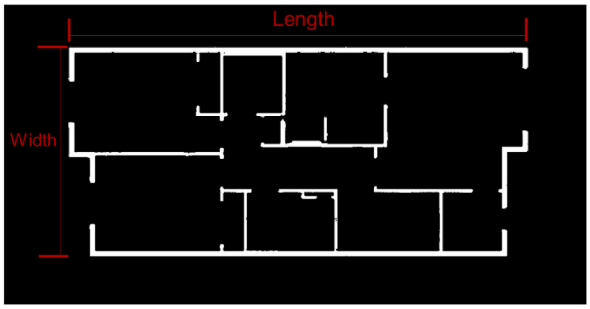


**Fig. 8.** Length and width for each floor.

(3), where $n$ is the number of data points, $x_i$ represents each data point and $c_j$ represents the center of the cluster to which $x_i$ is assigned. With each iteration, the center is adjusted until the distance is minimized. The cumulative distance is then quantified as the inertia.

$$I = \sum_{i=1}^{n} \|x_i - c_j\|^2 \tag{3}$$

### 3.3. Similarity assessment

To initiate the search for a target project, the first step is to determine its cluster classification. This classification streamlines the process by minimizing unnecessary comparisons. Since the centroids of each cluster are already determined, the nearest centroid identifies the appropriate cluster for the target project. Following cluster identification, the search for similar houses within the designated group involves computing difference metrics. This process entails comparing the target drawing with all drawings within the same cluster in the database. Subsequently, the similarity ratios (SR) were ranked to identify the top 10 best-matched houses. The SR was calculated as Eq. (4).

$$\mathrm{SR} = 1 - \frac{|\{y_T\} \cup \{y_D\}| - |\{y_T\} \cap \{y_D\}|}{|\{y_T\}|} \tag{4}$$

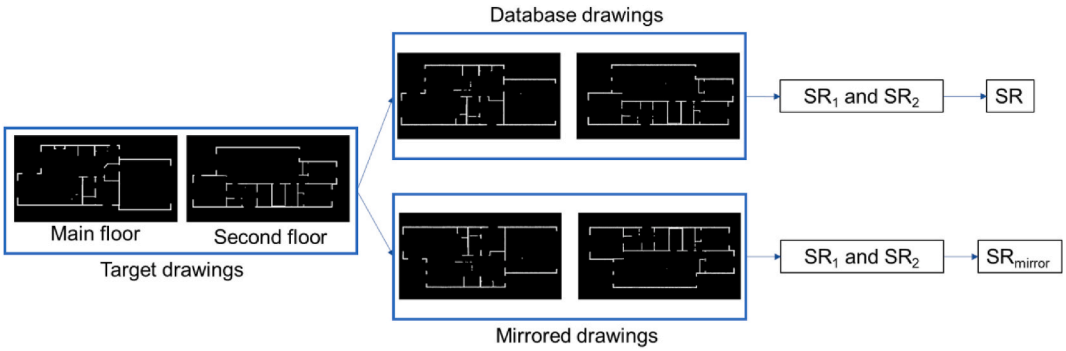


**Fig. 9.** The calculation step of SR and $SR_{mirror}$.

where $y_T$ is the set of pixels of the target project, and $y_D$ is the set of pixels of the project in the database.

The overall similarity ratio calculation steps are illustrated in Fig. 9. The main floor similarity ratio was calculated as $SR_1$, and the second-floor similarity ratio was described as $SR_2$. The overall SR is shown in Eq. (5).

$$SR = 0.5(SR_1 + SR_2) \tag{5}$$

In Eq. (5), SR was the average of $SR_1$ and $SR_2$. The weight is an adjustable factor and can be determined based on the data and experience. In this study, a fixed weight of 0.5 was applied to the similarity scores of the main and second floors to ensure equal contribution in the absence of specific design priorities. While this may not capture project-specific importance levels between floors, it serves as a reasonable baseline for general comparison.

Due to the possibility of drawings not being perfectly aligned, preprocessing steps were implemented before overlapping. If the scales of two drawings differ, the drawings must undergo resizing steps to ensure they share the same scale. The drawings were initially cropped from the left and top to align with the wall outlines, and the black areas were trimmed to ensure they shared the same dimensions, as illustrated in Fig. 10. This step ensures that the layouts are in the same location. Directly overlapping them without this adjustment might lead to low similarity ratios due to location differences, which would not accurately reflect their real distinctions. After overlapping, the drawings need to undergo morphological operations again to address any noisy points that may appear in the difference drawing. This step helps to ensure that only meaningful differences are highlighted, enhancing the accuracy and utility of the similarity assessment. Additionally, to accommodate mirror-drawing cases, a second value, $SR_{mirror}$, was calculated by vertically flipping the drawing. This vertical flipping addresses cases where the floor plans are mirrored, considering them as potentially best-matched houses as well. Subsequently, the final SR value was determined as the larger of the two values, as described in Eq. (6). Following an exhaustive search of all projects within a specific group, the SR values were ranked, with the top 10 largest values representing the search results. This comprehensive approach ensures that all potential matches, including mirrored layouts, are considered in the final analysis.

$$SR = max\{SR, SR_{mirror}\} \tag{6}$$

### 3.4. Highlight differences

The wall layout segmentation outcome primarily captures the shapes of the walls, but lacks additional contextual information. The clarity of pixel differences, which indicates the specific locations of these walls, is not distinct enough, making it difficult to clearly identify specific differences in wall locations. To overcome this limitation and improve the identification of variations for designers, an enhancement was introduced that highlights the differences directly in the original drawings. The process is illustrated in Fig. 11. First, the drawings were resized to their original dimensions, restoring for any previous cropping, as explained in Section 3.3. Then, the absolute difference in pixels was directly overlaid onto the original drawings, as shown visually in Fig. 11. This deliberate overlay was designed to highlight the points of differences, offering a clearer and more explicit representation of the variations in the house drawings.

Designers can leverage this augmented visualization to review the retrieved similar house drawings with highlighted differences. This not only facilitates a clearer understanding of the variations but also serves as a valuable point of reference for further analysis and decision-making in the design process. By emphasizing these differences, the augmented visualization enhances the interpretability of the visual data, helping designers make informed design choices based on the distinctions in wall layouts.

## 4. Case studies

To validate the accuracy of the proposed methodology, this section introduces two evaluation methods to assess its effectiveness. Firstly, case studies were conducted, featuring two categories: single-family prefabricated wood frame houses with detached and attached garages. Secondly, a human perception-based evaluation was employed, where individuals were invited to provide their opinions on the proposed method. This feedback helps gauge the practicality of the approach when applied to real-world scenarios.

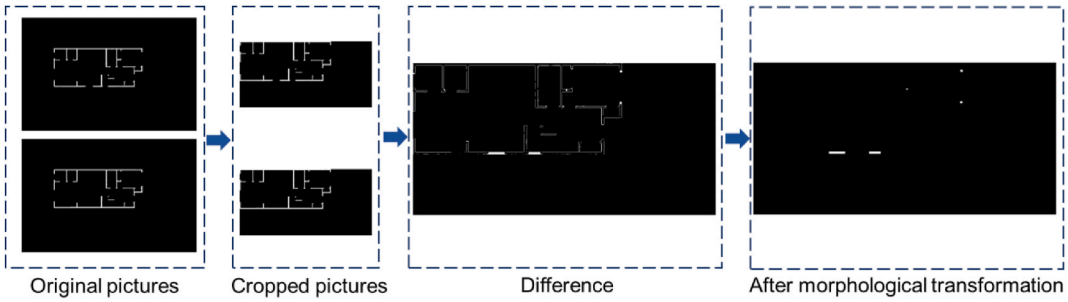


**Fig. 10.** Different pixels calculation process.

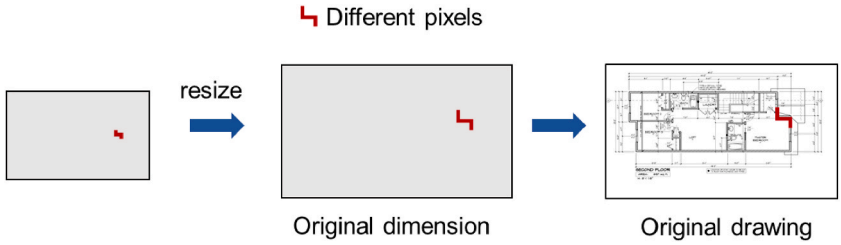


**Fig. 11.** Difference highlighting steps.

### 4.1. Database creation

The mIoU for the test dataset is 0.872. Fig. 12 shows the IoU of each drawing in the test dataset, with a mean IoU of 0.872 and a standard deviation of 0.048. Given that this IoU value is greater than related research [18], the performance of this model is satisfactory.

If the drawings are not at the same scale, they should undergo a scaling standardization process to ensure consistency. This allows for accurate comparison and prevents scaling-related issues during subsequent search and analysis. After gathering data from all the houses, the actual dimensions for the main floor and the second floor are depicted in Fig. 13. Each point represents one house. In Fig. 13, the dimensions exhibit a notable variation, which can be attributed to two primary factors. Firstly, houses with attached garages tend to have larger dimensions than those with detached garages. Secondly, variations in house layouts contribute to differences in dimensions.

In the application of K-means clustering, the determination of an appropriate number of clusters is crucial. To identify the most suitable number, Fig. 14 visualizes the relationship between various cluster numbers and the inertia of the clusters. Using the elbow method, it was determined that three clusters were optimal for the dataset. The distribution among these clusters is illustrated in Fig. 15, showing that Cluster 2 comprised the largest percentage at 42.7 %, followed by Cluster 3 and Cluster 1. The clustering primarily reflects the house type, with attached garage houses and detached garage houses placed in different clusters due to their significant dimension differences.

Following the clustering process, the tasks can be efficiently categorized into the relevant group, eliminating the need to search through the entire database. This refined approach not only enhances operational efficiency but also provides a more targeted and resource-effective strategy for subsequent tasks.

### 4.2. Analysis

In Fig. 16, two target houses underwent initial processing using the segmentation model to extract the wall layout. Subsequently, for the first case (houses with detached garage), the actual dimensions were computed as 46 by 20 feet for the main floor and 48 by 20 feet for the second floor. This particular configuration belongs to Cluster No. 3, which includes a total of 135 houses. In the second case, the total width and length dimensions were measured as 66 by 28 feet for the main floor and 62 by 26 feet for the second floor, placing it within Cluster No. 2.

After comparing all the drawings within the cluster by overlapping pictures to calculate the different pixel ratios, the similarity ratios for the ten best-matched houses were determined, which are visually presented in Fig. 17. The runtimes for the two cases are

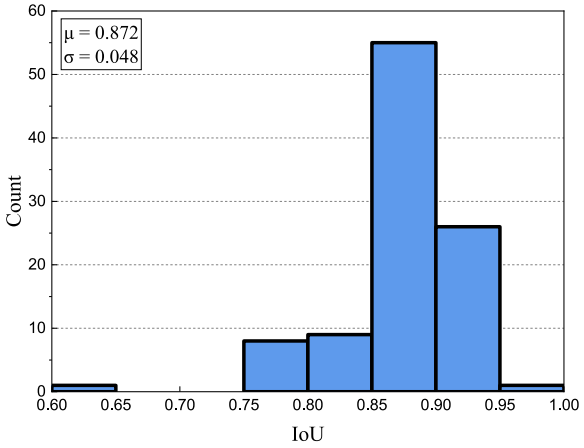


**Fig. 12.** IoU of all drawings in the test dataset.

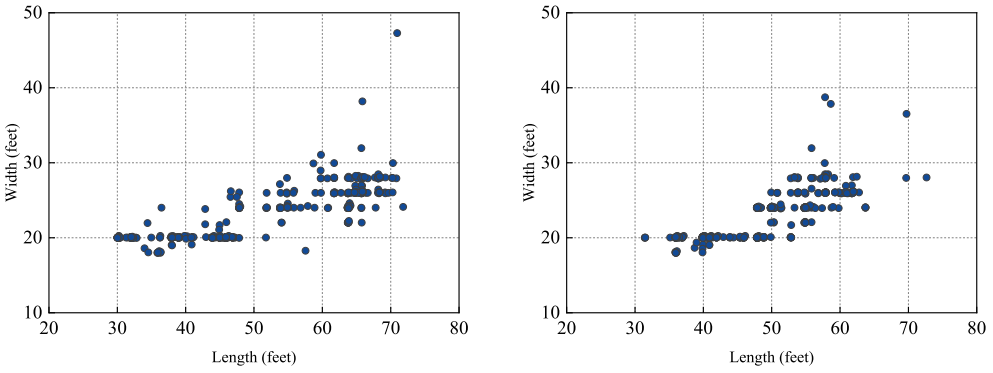


(a) Main floor (b) Second floor

**Fig. 13.** Dimensions of the main floor and the second floor.

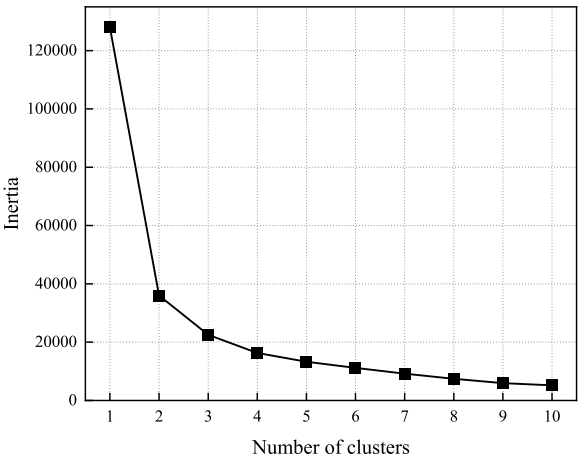


**Fig. 14.** Determination of number of clusters.

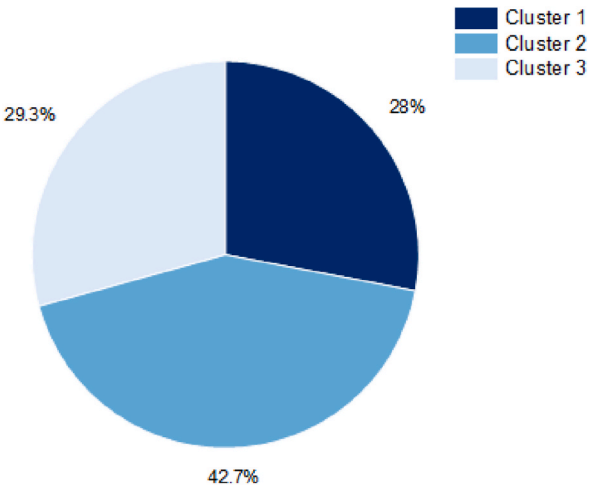


**Fig. 15.** Statistics for each cluster.

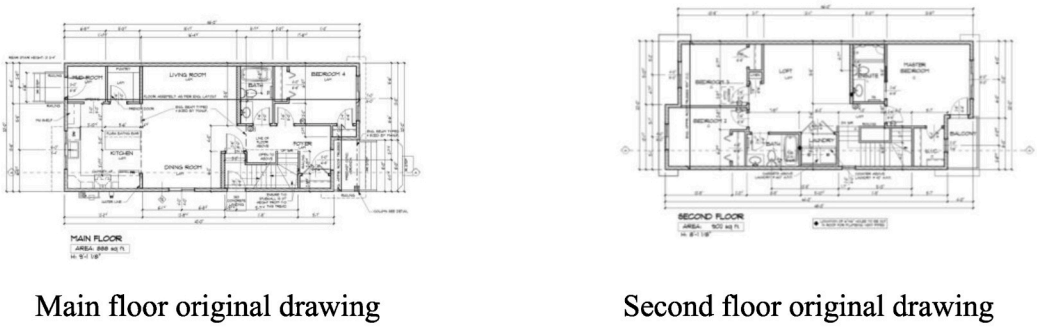


**Fig. 16.** Layout drawings for two cases.

83.9 s and 122.0 s, respectively. In Case 1, the five best-matched houses (from No. 1 to No. 5) exhibited relatively high similarity ratios (SR) of 98.1 %, 98.0 %, 97.8 %, 95.3 % and 93.9 %, respectively. This indicates a strong resemblance and consistency among these houses in terms of architectural features and layout. The five best matched houses for Case 1 are presented in Fig. 18. In Case 2, as shown in Fig. 17 (b), similarity ratios were lower compared to Case 1. The top five houses in this scenario showed similarity ratios of 89.8 %, 84.8 %, 79.0 %, 77.7 % and 77.6 %, respectively. The decreased similarity ratios in Case 2 underscore the distinct challenges encountered in finding closely matched houses. The five best-matched houses for Case 2 are presented in Fig. 19. The specific nature of modifications, particularly alterations to wall details, contributed to the decrease in similarity ratios, highlighting the sensitivity of similarity assessments to specific changes in architectural elements.

In Fig. 20, the differences between the target house and the matched houses are highlighted, illustrating the distinctions between them. Red areas indicate differences between the two drawings, where features in one drawing are absent in the other. It is worth noting that in Case 1, as shown in Fig. 20(a), the matched houses display very similar layouts, with only minor differences noted in the openings. There are differences in the openings on the main floor, indicating a potential variation in the opening's dimension

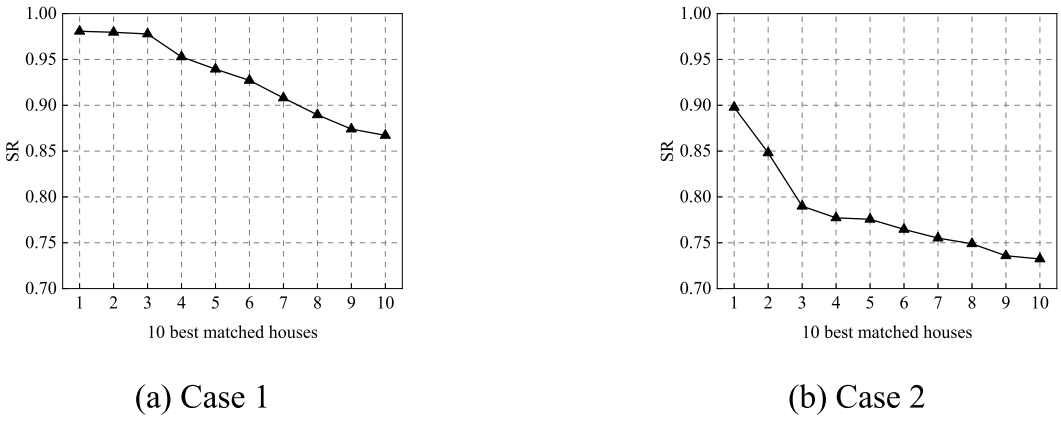


**Fig. 17.** Similarity ratio (SR) values for 10 best matched houses.

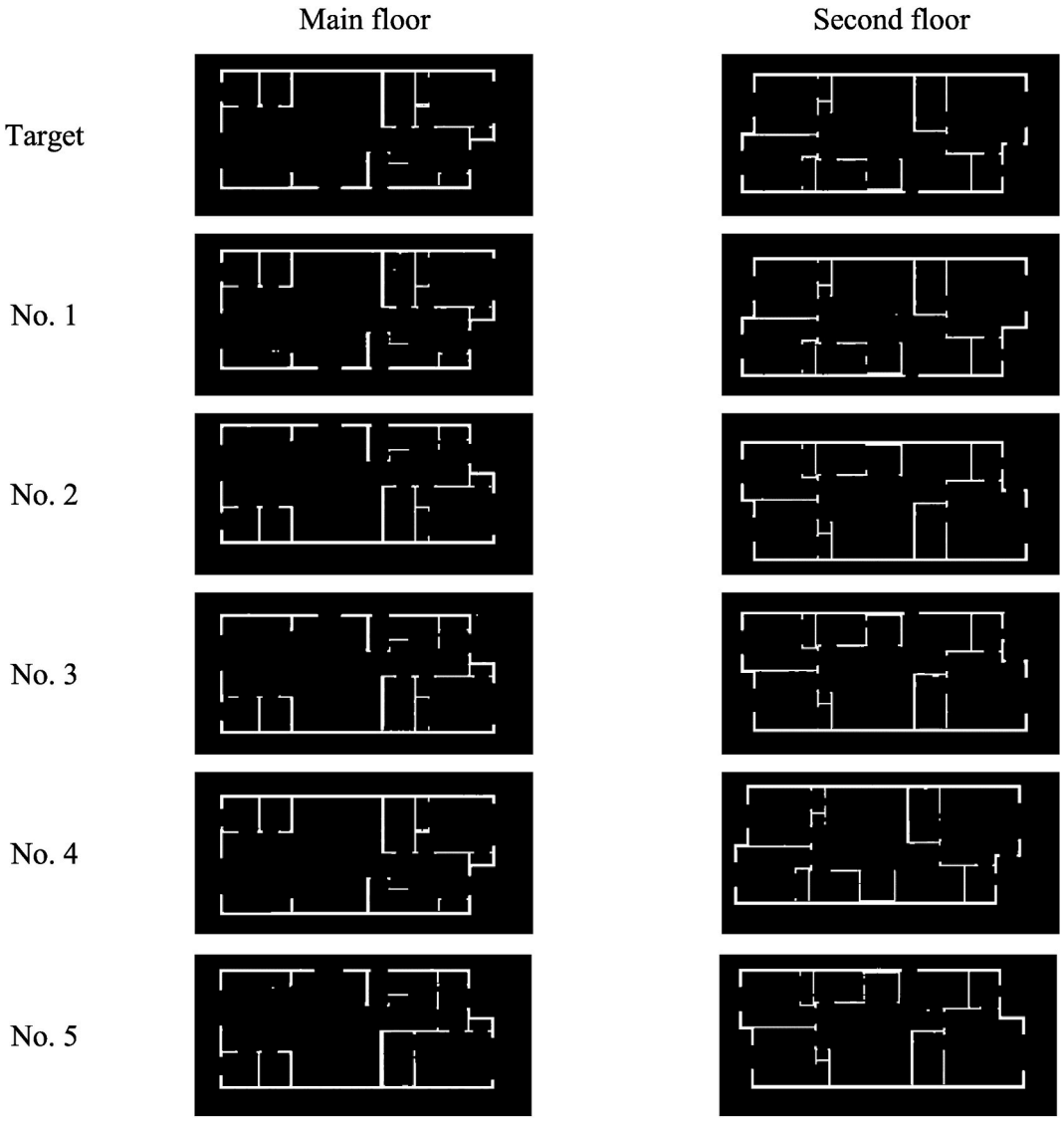


**Fig. 18.** Five best matched houses for Case 1.

compared to the previous model. In the second-floor result, the differences highlighted include wall and openings. Based on this, designers can focus on modifying these red areas to refine the layout model. Fig. 20(b) reveals more pronounced differences. For example, on the second floor, the red-highlighted areas indicate potential discrepancies in opening dimensions that need to be checked. For other red-highlighted areas, designers need to manually review these highlighted areas and make necessary modifications to the previous model. This detailed analysis assists in pinpointing specific areas for modification, enabling more precise and targeted improvements in the design process.

To obtain quantitative results for the difference highlighting, it is essential to compare the results with ground truth data. Ground truth data represents the outcomes from the comparison of manually annotated wall outlines, used to identify the different pixels rather than relying on the pictures segmented by the model, as shown in Fig. 21. This approach ensures that the evaluation is based on the most accurate and relevant differences between the actual layouts and the model's interpretations. Since the IoU metric may not fully capture all aspects of the results, it was not used to quantify the results in this instance. Instead, the metrics used to quantify the results include recall and precision, which are defined in Eqs. (7) and (8). TP (True Positives) refers to the number of true white pixels correctly identified, and FN (False Negatives) is the number of false black pixels, representing true positives that were missed. FP (False Positives) are the false white pixels, indicating negatives that were incorrectly identified as positives. The results for the five best-matched houses are shown in Table 1.

$$\text{Recall} = \frac{TP}{TP + FN} \tag{7}$$

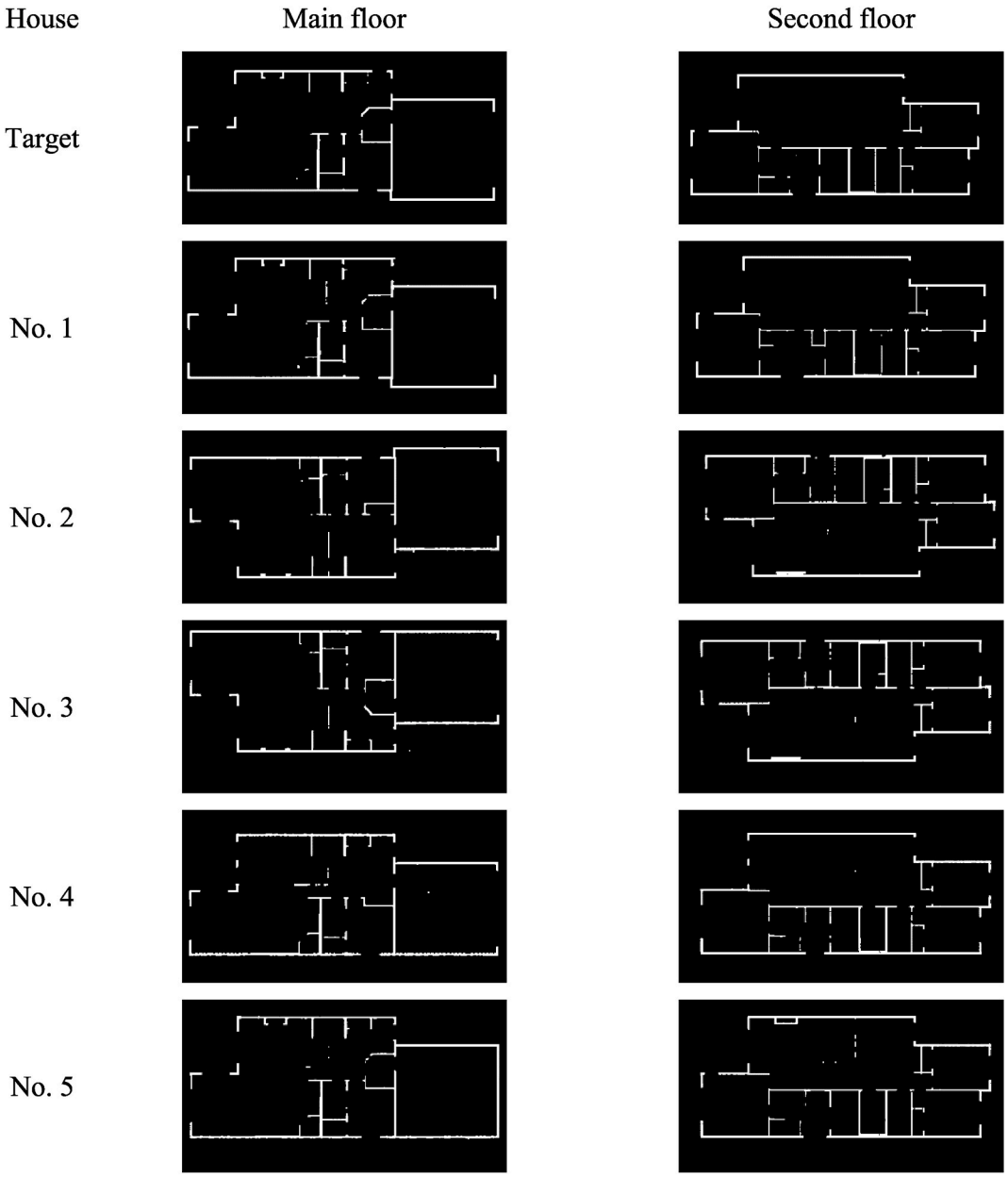


**Fig. 19.** Five best matched houses for Case 2.

$$\text{Precision} = \frac{TP}{TP + FP} \tag{8}$$

In Table 1, which detail the evaluation results for two cases, the data shows high recall values. This indicates the model is effective at detecting nearly all differences, which is crucial for ensuring that designers do not overlook any potential modifications. However, the precision values are lower, which may be attributed to two main factors: errors from the segmentation process and the limited number of white ground truth pixels in some scenarios. The low precision indicates that while the model is effective at identifying many areas of difference, some of these highlighted differences may not be accurate, leading to false positives. This is evident in cases where the number of actual differences (white pixels) is small, making each false positive more impactful on the precision metric. Despite this, the higher recall value is beneficial in this context since it ensures that designers will miss few critical areas when modifying the previous models. This conservative approach favors ensuring all potential differences are reviewed, even at the cost of examining some areas that do not require changes, which is a preferable strategy in precision-sensitive tasks.

Based on these results, designers have the option to select a previously completed house and initiate the entire design process by

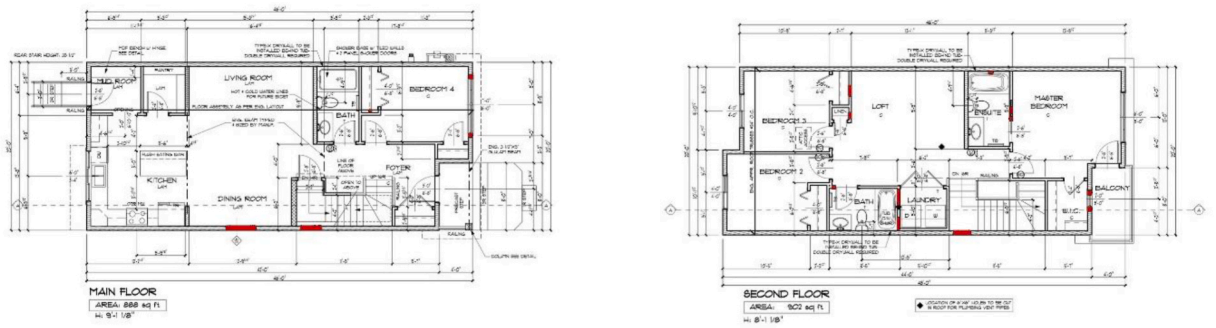


(a) Case 1 (Ranking 4)

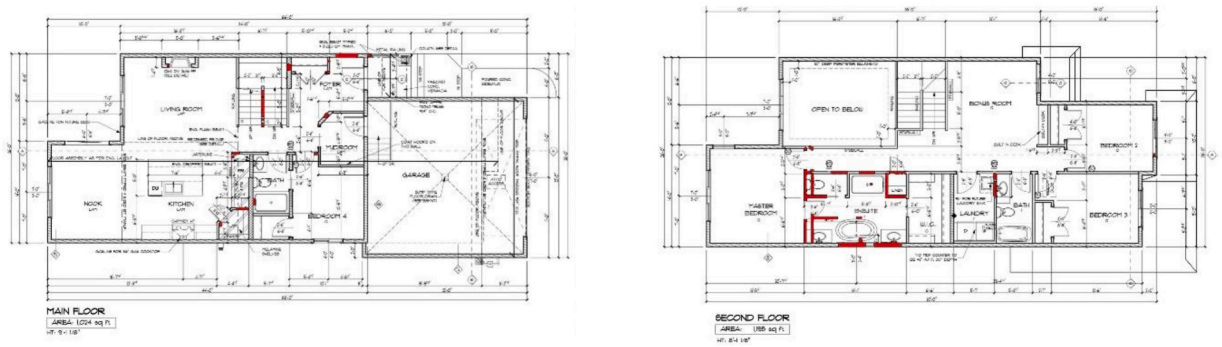


(b) Case 2 (Ranking 1)

**Fig. 20.** Visualization of differences between the target house and the matched house on the main floor drawing (left) and the second floor drawing (right).

making necessary modifications to the chosen house. Each red area highlighted in the results needs to be carefully inspected by designers to verify the differences and make appropriate modifications. It is also important to note that small red areas may appear in the final result due to segmentation errors. To ensure the safety and reliability of the results, caution should be exercised when considering these false red pixels in the final output. This strategy allows for a comprehensive examination by human designers, reducing the risk of overlooking any potential discrepancies. Additionally, the study emphasizes that differences in wall configurations are critical, as walls often serve as foundational elements influencing other types of variations in the final results. Using an existing house as a starting point and adjusting as necessary can significantly enhance efficiency. Designers will focus on the red areas, implementing changes such as enlarging or reducing openings, relocating walls, or adjusting wall dimensions in the new house. By making these targeted adjustments, the analysis process becomes quicker, more efficient, and tailored to specific needs, thereby optimizing the overall design workflow.

### *4.3. Perception-based evaluation*

Evaluating the accuracy of similarity searches in engineering drawings can be complex, as it involves both objective and subjective elements. To address this, the study involved ten participants with backgrounds in civil engineering to evaluate the feasibility of the proposed method. Each participant was tasked with independently selecting what they considered to be the three best-matched houses based on their professional judgment and expertise. The evaluation criteria were based on how closely the participants' rankings aligned with the rankings produced by the methodology. In each case, ten houses were presented, labelled from 1 to 10, with 1 representing the top-ranked result by the proposed method and 10 the tenth. For example, if a participant's top three choices were 1, 2, and 4, the scores assigned would be 1, 2, and 4, respectively. These scores were then used to gauge how well the participants' evaluation corresponded with the computational rankings.

The results of this subjective evaluation are detailed in Table 2. For each case, the rankings generated by the proposed method were compared to the average rankings from the human evaluators, and the differences were calculated. The findings indicate that the results by the proposed method are quite similar to human decisions, with discrepancies ranging from 0.9 to 1.7. These differences are relatively minor and are considered acceptable within the context of engineering evaluations. Such variance is manageable as designers typically review all potential matches and select the most suitable option based on a comprehensive assessment of each case.

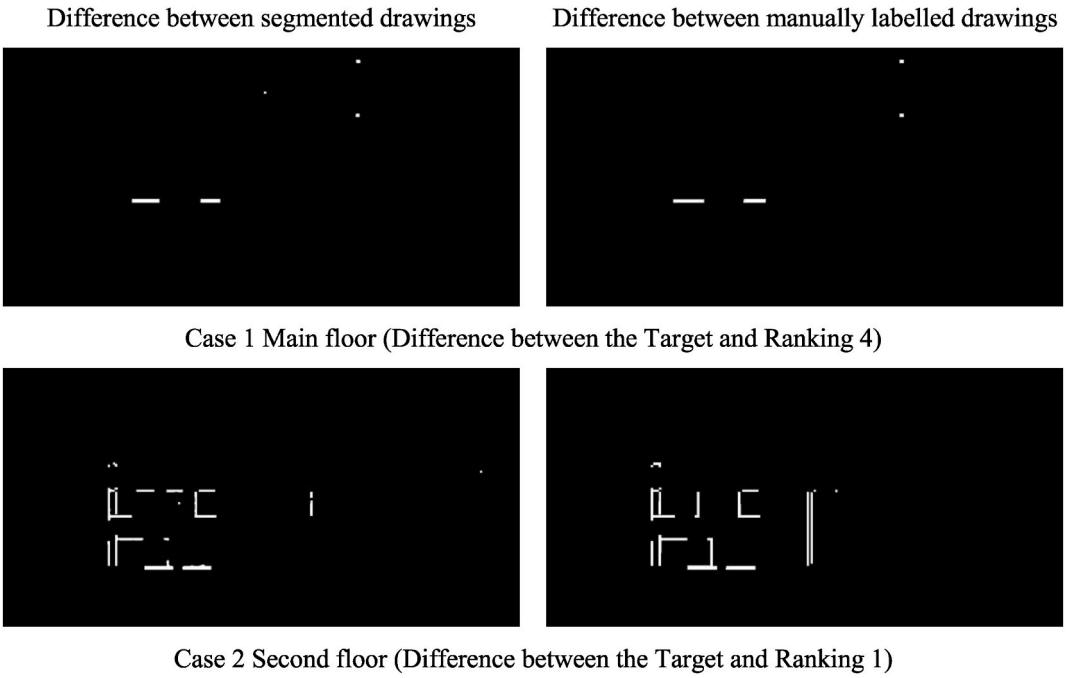


**Fig. 21.** Differences between two segmented drawings and two manually labelled drawings.

**Table 1**
Accuracy of highlighting differences for two cases for the five best matched houses.

| Case | Main floor | | Second floor | |
|---|---|---|---|---|
| | Recall | Precision | Recall | Precision |
| #1 | 0.68 | 0.40 | 0.85 | 0.36 |
| #2 | 0.81 | 0.63 | 0.65 | 0.46 |

**Table 2**
Comparison between proposed method-generated results and human scores for two cases.

| Ranking by the proposed method | Case 1 | Case 2 |
|---|---|---|
| | Average human score | Average human score |
| 1 | 2.3 | 2.7 |
| 2 | 2.9 | 3.3 |
| 3 | 4.7 | 4.2 |

## 5. Discussion

### 5.1. Method comparison

To compare the segmentation performance, U-Net [17] and Attention U-Net [43] were selected as baselines. Swin UNETR [36] achieved the highest IoU of 0.872, showing an improvement over U-Net (0.841) and Attention U-Net (0.863). These results demonstrate the effective performance of the transformer-based model in segmenting walls in floor plan drawings.

The proposed method uses pixel difference as the main way to measure similarity. To compare with other methods, the Structural Similarity index (SSIM) [44] was also tested. The results are shown in Fig. 22. SSIM gives very high similarity values, but the goal is to find houses that are easy to modify. Pixel difference better reflects the actual effort needed to update the model. Although other metrics like SSIM can be used, the high similarity scores may lead to an underestimation of the modification workload.

### 5.2. Project clustering

To optimize the database search process, a K-means clustering algorithm was implemented, using dimensions as the primary

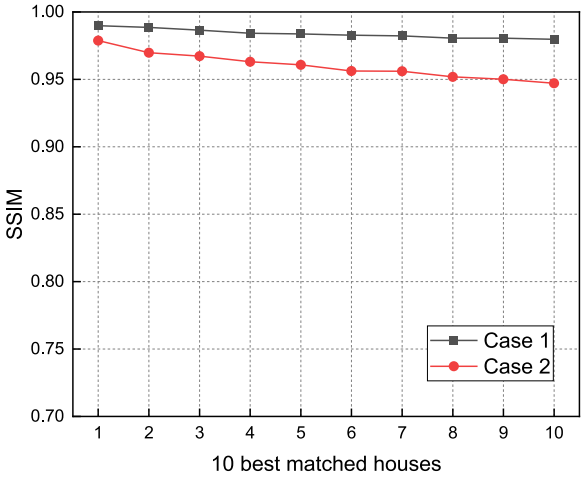


**Fig. 22.** 10 best matched houses using SSIM.

clustering variables. Dimensions are crucial for analyzing prefabricated timber houses, as they determine house areas, room layouts, and help differentiate house types—such as those with detached versus attached garages. For a new project, a convenient way to distinguish between a detached or attached garage is by examining the dimensions. Three clusters were selected in this study to balance runtime and performance. Using more clusters may reduce search time, as each cluster may contain fewer houses. The optimal number of clusters depends on the characteristics of the dataset. If the dataset includes not only single-family houses but also other building types, the variation in building dimensions increases, and more clusters may be needed to capture that variety.

Table 3 shows the search time for two cases, with and without clustering. By employing clustering, the search time decreases by over 50 %, despite yielding the same search results in both cases. The reduced search time is attributed to clustering, which avoids unnecessary image comparisons, thereby improving efficiency. Given the importance of dimensions in project comparisons, dimension-based clustering significantly enhances the search process.

K-means clustering was chosen to group buildings by size due to its simplicity, efficiency, and suitability for numerical data. K-means aims to partition n observations into k clusters by assigning each observation to the nearest cluster centroid [42]. To compare its performance, Gaussian Mixture Model (GMM) clustering [45] was also applied to the same dataset. The GMM produced three clusters, representing 8.7 %, 6.3 %, and 85 % of the data, respectively. When applying the GMM clustering results to the two test cases, Case 1 yielded the same outcome as K-means since it falls within the dominant 85 % cluster. However, Case 2 produced different results, as shown in Fig. 23, because it belongs to the 8.7 % cluster. This smaller cluster led to less effective retrieval compared to K-means. The choice of clustering methods largely depends on the dataset. Selecting an appropriate method can reduce search time while maintaining accuracy.

### 5.3. *Morphological operations*

Morphological operations are crucial throughout the process, from segmentation to difference highlighting. Noise points can appear due to various factors. First, segmentation may not accurately segment the wall due to the presence of complex symbols. Second, during difference highlighting, the absolute difference calculation may result in noisy outlines. This occurs because varying line thicknesses in different drawings can create slight boundary discrepancies in wall segmentation. Morphological operations help eliminate these unnecessary differences, as they result from line thickness variations that do not affect the overall wall dimensions or locations—key factors for designers.

The architectural layout serves as an initial design phase, while the detailed structural design depends on accurate wall dimensions and placements. However, morphological operations can slightly alter unclear wall segmentation results, as shown in Fig. 24. The walls may become fragmented into small discrete pieces after applying these operations. But this fragmentation does not affect the matching process, as the comparison is based on the overlap of the entire drawings. The error pixels from fragmentation account for only a small percentage of the total white pixels, making their impact negligible.

**Table 3**
Searching time for two cases with and without clustering (unit: s).

| Case | Without clustering | With clustering |
|---|---|---|
| 1 | 285.1 | 83.9 |
| 2 | 286.9 | 122.0 |

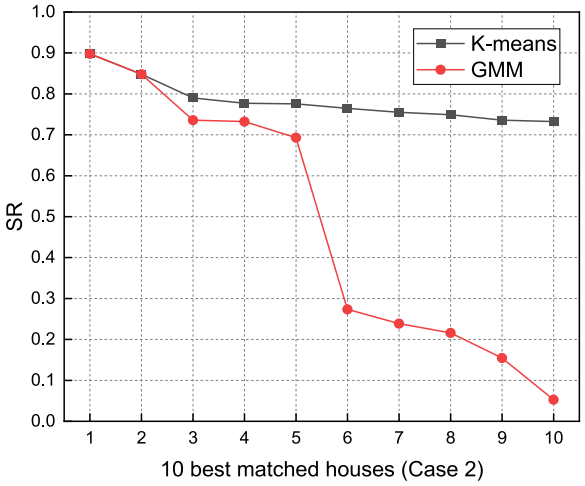


**Fig. 23.** Comparison of retrieval results using K-means and GMM clustering for Case 2.


**Fig. 24.** Segmented drawings without and with morphological operations.

### *5.4. Error analysis*

There are still segmentation errors that may affect the accuracy of the searching and comparison analysis. As shown in Fig. 25, a common error occurs when the features of interior walls are unclear. Given this limitation, it remains essential for designers to manually verify the final comparison results to ensure accuracy.

## 6. Conclusions and future work

This study introduces a systematic method designed to enhance the efficiency of designers in searching existing databases to

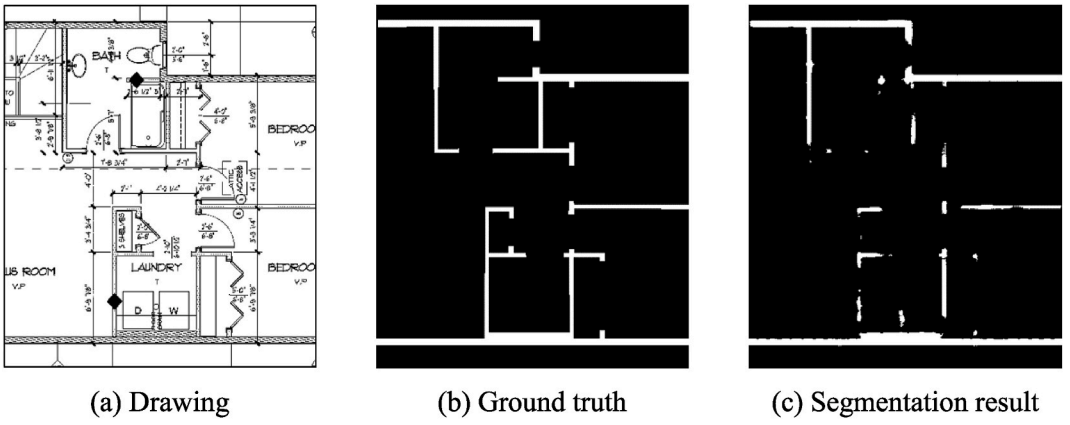


**Fig. 25.** Error analysis in segmentation.

identify and modify previous housing construction projects by retrieving similar drawings and highlighting differences. The proposed method is centered on the creation of a dimension-based database that is clustered to facilitate search and comparison, with differences clearly highlighted between the best-matched projects. The main conclusions are summarized as follows.

1) The database can be built based on segmenting the layout drawings. Morphological operations can further improve the post-processing of segmented drawings for removing noise points during the whole process.
2) The similarity assessment method simplifies the comparison of wall drawings through direct dimensional analysis and drawing manipulation techniques like cropping and resizing. This systematic approach enhances the identification of closely matched buildings.
3) Differences between drawings are detected and highlighted by overlapping pre-processed drawings, which improves the understanding of variations. This is crucial for model modifications during the drafting stage.

This research presents an innovative approach to examining differences in layout drawings, specifically focusing on variations in wall locations and dimensions. The objective is to assist designers in modifying previously completed projects rather than initiating entirely new designs. However, the study acknowledges certain limitations. The focus on wall differences does not encompass all aspects of model modifications, such as materials and elevation details, indicating the need for more comprehensive information in future enhancements. Additionally, the dataset is tailored to a specific aspect of prefabricated buildings with uniform scaling, emphasizing similarities in wood-frame structures. In the future, incorporating a wider variety of drawing types in the segmentation process will be considered. Utilizing more diverse drawings is expected to improve the model's ability to generalize across different building styles and structural systems.

The current similarity and difference-highlighting methods rely solely on 2D plan drawings, which do not capture important spatial, structural, or elevation-specific aspects present in 3D models. This limitation may result in missing significant differences in practical applications where 3D variations play a critical role. To address this, future research will focus on integrating BIM data, which provide richer information across floors and elevations. Such integration will enable more accurate change detection and support more comprehensive retrieval, design comparison, and construction planning processes.

This study demonstrates the effectiveness of wall segmentation using the specific model. Performance improvements using new state-of-the-art models with the best performance will be explored in future work. Future work will also aim to include additional experiments to benchmark the framework using state-of-the-art segmentation models to further validate its performance and extend its applicability to a broader range of scenarios. Diffusion models also represent a future direction for architectural drawing-related tasks. Since drawings are typically available in various formats [46], this will include evaluating its effectiveness across diverse databases to ensure its practicality for various building types. With more industrial feedback, the weights of different floors can also be adaptively adjusted to better reflect project-specific priorities and functional differences can be further explored. By integrating 3D modeling considerations and refining the methodology, future research will contribute to more effective tools for designers, improving both modification processes and the adaptation of existing designs to new contexts.

## CRediT authorship contribution statement

**Hao Xie:** Writing – review & editing, Writing – original draft, Visualization, Validation, Software, Methodology, Investigation, Formal analysis, Conceptualization. **Qipei Mei:** Writing – review & editing, Supervision, Investigation, Funding acquisition, Conceptualization. **Ying Hei Chui:** Writing – review & editing, Supervision, Investigation, Funding acquisition. **Haitao Yu:** Writing – review & editing, Supervision, Resources, Conceptualization.

## Declaration of competing interest

The authors declare that they have no known competing financial interests or personal relationships that could have appeared to influence the work reported in this paper.

## Acknowledgements

The authors would like to acknowledge the funding support provided by Natural Sciences and Engineering Research Council (NSERC) of Canada through its Alliance Grant program [ALLRP(581074-22)], Alberta Innovates (212201668) and Landmark Group of Companies Inc.

## Data availability

The authors do not have permission to share data.

## References

[1] S. Navaratnam, T. Ngo, T. Gunawardena, D. Henderson, Performance review of prefabricated building systems and future research in Australia, Buildings 9 (2019) 38, https://doi.org/10.3390/buildings9020038.

[2] H. Wang, Y. Zhang, W. Gao, S. Kuroki, Life cycle environmental and cost performance of prefabricated buildings, Sustainability 12 (2020) 2609, https://doi.org/10.3390/su12072609.
[3] W. Liao, X. Lu, Y. Huang, Z. Zheng, Y. Lin, Automated structural design of shear wall residential buildings using generative adversarial networks, Autom. ConStruct. 132 (2021) 103931, https://doi.org/10.1016/j.autcon.2021.103931.
[4] W. Liao, Y. Huang, Z. Zheng, X. Lu, Intelligent generative structural design method for shear wall building based on "fused-text-image-to-image" generative adversarial networks, Expert Syst. Appl. 210 (2022) 118530, https://doi.org/10.1016/j.eswa.2022.118530.
[5] Y. Fei, W. Liao, S. Zhang, P. Yin, B. Han, P. Zhao, X. Chen, X. Lu, Integrated schematic design method for shear Wall structures: a practical application of generative adversarial networks, Buildings 12 (2022) 1295, https://doi.org/10.3390/buildings12091295.
[6] P. Zhao, W. Liao, Y. Huang, X. Lu, Intelligent design of shear wall layout based on attention-enhanced generative adversarial network, Eng. Struct. 274 (2023) 115170, https://doi.org/10.1016/j.engstruct.2022.115170.
[7] Y. Gu, Y. Huang, W. Liao, X. Lu, Intelligent design of shear wall layout based on diffusion models, Comput. Aided Civ. Infrastruct. Eng. (2024), https://doi.org/10.1111/mice.13236 mice.13236.
[8] Y. Zhou, H. Leng, S. Meng, H. Wu, Z. Zhang, StructDiffusion: end-to-end intelligent shear wall structure layout generation and analysis using diffusion model, Eng. Struct. 309 (2024) 118068, https://doi.org/10.1016/j.engstruct.2024.118068.
[9] Y. Fei, W. Liao, Y. Huang, X. Lu, Knowledge-enhanced generative adversarial networks for schematic design of framed tube structures, Autom. ConStruct. 144 (2022) 104619, https://doi.org/10.1016/j.autcon.2022.104619.
[10] P. Zhao, W. Liao, H. Xue, X. Lu, Intelligent design method for beam and slab of shear wall structure based on deep learning, J. Build. Eng. 57 (2022) 104838, https://doi.org/10.1016/j.jobe.2022.104838.
[11] P. Zhao, W. Liao, Y. Huang, X. Lu, Intelligent beam layout design for frame structure based on graph neural networks, J. Build. Eng. 63 (2023) 105499, https://doi.org/10.1016/j.jobe.2022.105499.
[12] B. Fu, Y. Gao, W. Wang, Dual generative adversarial networks for automated component layout design of steel frame-brace structures, Autom. ConStruct. 146 (2023) 104661, https://doi.org/10.1016/j.autcon.2022.104661.
[13] B. Fu, W. Wang, Y. Gao, Physical rule-guided generative adversarial network for automated structural layout design of steel frame-brace structures, J. Build. Eng. 86 (2024) 108943, https://doi.org/10.1016/j.jobe.2024.108943.
[14] B. Yang, B. Liu, D. Zhu, B. Zhang, Z. Wang, K. Lei, Semiautomatic structural BIM-model generation methodology using CAD construction drawings, J. Comput. Civ. Eng. 34 (2020) 04020006, https://doi.org/10.1061/(ASCE)CP.1943-5487.0000885.
[15] L. Gimenez, S. Robert, F. Suard, K. Zreik, Automatic reconstruction of 3D building models from scanned 2D floor plans, Autom. ConStruct. 63 (2016) 48–56, https://doi.org/10.1016/j.autcon.2015.12.008.
[16] P.N. Pizarro, N. Hitschfeld, I. Sipiran, J.M. Saavedra, Automatic floor plan analysis and recognition, Autom. ConStruct. 140 (2022) 104348, https://doi.org/10.1016/j.autcon.2022.104348.
[17] O. Ronneberger, P. Fischer, T. Brox, U-Net: Convolutional networks for biomedical image segmentation, in: N. Navab, J. Hornegger, W.M. Wells, A.F. Frangi (Eds.), Med. Image Comput. Comput.-Assist. Interv. – MICCAI 2015, Springer International Publishing, Cham, 2015, pp. 234–241, https://doi.org/10.1007/978-3-319-24574-4_28.
[18] P.N. Pizarro, N. Hitschfeld, I. Sipiran, Large-scale multi-unit floor plan dataset for architectural plan analysis and recognition, Autom. ConStruct. 156 (2023) 105132, https://doi.org/10.1016/j.autcon.2023.105132.
[19] Z. Zeng, X. Li, Y.K. Yu, C.-W. Fu, Deep floor plan recognition using a multi-task network with room-boundary-guided attention, in: 2019 IEEECVF Int. Conf. Comput. Vis. ICCV, IEEE, Seoul, Korea (South), 2019, pp. 9095–9103, https://doi.org/10.1109/ICCV.2019.00919.
[20] Y. Zhao, X. Deng, H. Lai, Reconstructing BIM from 2D structural drawings for existing buildings, Autom. ConStruct. 128 (2021) 103750, https://doi.org/10.1016/j.autcon.2021.103750.
[21] S. Ren, K. He, R. Girshick, J. Sun, Faster R-CNN: towards real-time object detection with region proposal networks, IEEE Trans. Pattern Anal. Mach. Intell. 39 (2017) 1137–1149, https://doi.org/10.1109/TPAMI.2016.2577031.
[22] C. Liu, P. Kohli, J. Wu, Y. Furukawa, Raster-to-Vector: revisiting floorplan transformation, IEEE Int. Conf. Comput. Vis. (2017) 2195–2203, https://doi.org/10.1109/ICCV.2017.241.
[23] X. Lv, S. Zhao, X. Yu, B. Zhao, Residential floor plan recognition and reconstruction, in: 2021 IEEECVF Conf. Comput. Vis. Pattern Recognit. CVPR, IEEE, Nashville, TN, USA, 2021, pp. 16712–16721, https://doi.org/10.1109/CVPR46437.2021.01644.
[24] Z. Xu, N. Jha, S. Mehadi, M. Mandal, Multiscale object detection on complex architectural floor plans, Autom. ConStruct. 165 (2024) 105486, https://doi.org/10.1016/j.autcon.2024.105486.
[25] H. Xie, X. Ma, Q. Mei, Y.H. Chui, A semi-supervised approach for building wall layout segmentation based on transformers and limited data, Comput. Aided Civ. Infrastruct. Eng. (2024), https://doi.org/10.1111/mice.13397 mice.13397.
[26] H. Chu, D. Yu, W. Chen, J. Ma, L. Deng, A rendering-based lightweight network for segmentation of high-resolution crack images, Comput. Aided Civ. Infrastruct. Eng. (2024), https://doi.org/10.1111/mice.13290 mice.13290.
[27] J.H. Park, B.S. Um, A new approach to similarity retrieval of 2-D graphic objects based on dominant shapes, Pattern Recognit. Lett. 20 (1999) 591–616, https://doi.org/10.1016/S0167-8655(99)00022-7.
[28] M.J. Fonseca, J.A. Jorge, Towards content-based retrieval of technical drawings through high-dimensional indexing, Comput. Graph. 27 (2003) 61–69, https://doi.org/10.1016/S0097-8493(02)00244-3.
[29] W. Yu, J. Hsu, Content-based text mining technique for retrieval of CAD documents, Autom. ConStruct. 31 (2013) 65–74, https://doi.org/10.1016/j.autcon.2012.11.037.
[30] D. Sharma, N. Gupta, C. Chattopadhyay, S. Mehta, DANIEL: a deep architecture for automatic analysis and retrieval of building floor plans, in: 2017 14th IAPR Int. Conf. Doc. Anal. Recognit. ICDAR, IEEE, Kyoto, 2017, pp. 420–425, https://doi.org/10.1109/ICDAR.2017.76.
[31] R. Khade, K. Jariwala, C. Chattopadhyay, U. Pal, A rotation and scale invariant approach for multi-oriented floor plan image retrieval, Pattern Recognit. Lett. 145 (2021) 1–7, https://doi.org/10.1016/j.patrec.2021.01.020.
[32] A. Kalsekar, R. Khade, K. Jariwala, C. Chattopadhyay, RISC-net : rotation invariant siamese convolution network for floor plan image retrieval, Multimed. Tool. Appl. 81 (2022) 41199–41223, https://doi.org/10.1007/s11042-022-13124-3.
[33] R. Xiao, Comparing and clustering residential layouts using a novel measure of grating difference, Nexus Netw. J. 23 (2021) 187–208, https://doi.org/10.1007/s00004-020-00530-z.
[34] E. Rodrigues, D. Sousa-Rodrigues, M. Teixeira de Sampayo, A.R. Gaspar, Á. Gomes, C. Henggeler Antunes, Clustering of architectural floor plans: a comparison of shape representations, Autom. ConStruct. 80 (2017) 48–65, https://doi.org/10.1016/j.autcon.2017.03.017.
[35] C.C.J. Van Engelenburg, S. Khademi, J.C. Van Gemert, SSIG: a visually-guided graph edit distance for floor plan similarity, in: 2023 IEEECVF Int. Conf. Comput. Vis. Workshop ICCVW, IEEE, Paris, France, 2023, pp. 1565–1574, https://doi.org/10.1109/ICCVW60793.2023.00172.
[36] A. Hatamizadeh, V. Nath, Y. Tang, D. Yang, H.R. Roth, D. Xu, Swin UNETR: swin transformers for semantic segmentation of brain tumors in MRI images, in: A. Crimi, S. Bakas (Eds.), Brainlesion Glioma Mult. Scler. Stroke Trauma. Brain Inj., Springer International Publishing, Cham, 2022, pp. 272–284, https://doi.org/10.1007/978-3-031-08999-2_22.
[37] C. Harris, M. Stephens, A combined corner and edge detector, in: Procedings Alvey Vis. Conf. 1988, Alvey Vision Club, Manchester, 1988, pp. 23.1–23.6, https://doi.org/10.5244/C.2.23.
[38] T.-Y. Lin, P. Goyal, R. Girshick, K. He, P. Dollar, Focal loss for dense object detection, in: 2017 IEEE Int. Conf. Comput. Vis. ICCV, IEEE, Venice, 2017, pp. 2999–3007, https://doi.org/10.1109/ICCV.2017.324.
[39] Q. Mei, M. Gül, A cost effective solution for pavement crack inspection using cameras and deep neural networks, Constr. Build. Mater. 256 (2020) 119397, https://doi.org/10.1016/j.conbuildmat.2020.119397.

[40] T. Yamaguchi, T. Mizutani, Quantitative road crack evaluation by a U-Net architecture using smartphone images and Lidar data, Comput. Aided Civ. Infrastruct. Eng. 39 (2024) 963–982, https://doi.org/10.1111/mice.13071.
[41] R.M. Haralick, S.R. Sternberg, X. Zhuang, Image analysis using mathematical morphology, IEEE Trans. Pattern Anal. Mach. Intell. (1987) 532–550, https://doi.org/10.1109/TPAMI.1987.4767941. PAMI-9.
[42] A.K. Jain, Data clustering: 50 years beyond K-means, Pattern Recognit. Lett. 31 (2010) 651–666. https://doi.org/10.1016/j.patrec.2009.09.011.
[43] O. Oktay, J. Schlemper, L.L. Folgoc, M. Lee, M. Heinrich, K. Misawa, K. Mori, S. McDonagh, N.Y. Hammerla, B. Kainz, B. Glocker, D. Rueckert, Attention U-Net: Learning Where to Look for the Pancreas, 2018. http://arxiv.org/abs/1804.03999. (Accessed 1 August 2024).
[44] Zhou Wang, A.C. Bovik, H.R. Sheikh, E.P. Simoncelli, Image quality assessment: from error visibility to structural similarity, IEEE Trans. Image Process. 13 (2004) 600–612, https://doi.org/10.1109/TIP.2003.819861.
[45] E. Patel, D.S. Kushwaha, Clustering cloud workloads: K-Means vs gaussian mixture model, Procedia Comput. Sci. 171 (2020) 158–167, https://doi.org/10.1016/j.procs.2020.04.017.
[46] S. Kim, S. Park, H. Kim, K. Yu, Deep floor plan analysis for complicated drawings based on style transfer, J. Comput. Civ. Eng. 35 (2021) 04020066, https://doi.org/10.1061/(ASCE)CP.1943-5487.0000942.